Available online at www.sciencedirect.com
SCIENCE DIRECT
Earth and Planetary Science Letters 244 (2006) 639–654
EPSL
www.elsevier.com/locate/epsl

Seismic activity in the Sumatra–Java region prior to the December 26, 2004 (M_w=9.0–9.3) and March 28, 2005 (M_w=8.7) earthquakes

Arnaud Mignan [a], Geoffrey King [a,*], David Bowman [b], Robin Lacassin [a], Renata Dmowska [c]

[a] *Institut de Physique du Globe de Paris, Laboratoire de Tectonique et de Mécanique de la Lithosphère, 4, place Jussieu, 75252 Paris. Cedex 5, France*
[b] *Department of Geological Sciences, California State University Fullerton, 800 State College Blvd., Fullerton, CA 92834-6850, USA*
[c] *Division of Engineering and Applied Sciences, Harvard University, 29 Oxford St., Cambridge, MA 02138, USA*

Received 7 July 2005; received in revised form 26 January 2006; accepted 26 January 2006
Available online 13 March 2006
Editor: V. Courtillot

Abstract

A promising approach to assessing seismic hazards has been to combine the concept of seismic gaps with Coulomb-stress change modeling to refine short-term earthquake probability estimates. However, in practice the large uncertainties in the seismic histories of most tectonically active regions limit this approach since a stress increase is only important when a fault is already close to failure. In contrast, recent work has suggested that Accelerated Moment Release (AMR) can help to identify when a stretch of fault is approaching failure without any knowledge of the seismic history of the region. AMR can be identified in the regions around the Sumatra Subduction system that must have been stressed before the 26 December 2004 and 28 March 2005 earthquakes. The effect is clearest for the epicentral regions with less than a 2% probability that it could occur in a random catalogue. Less clear AMR is associated with the regions north of Sumatra around the Nicobar and Andaman islands where rupture in the December 2004 earthquake was less vigorous. No AMR is found for the region of the 1833 Sumatran earthquake suggesting that an event in this region in the near future is unlikely. AMR similar to that before the December 2004 and March 2005 events is found for a 750 km stretch of the southeastern Sumatra and western Java subduction system suggesting that it is close to failure. Should the whole of this stretch break in a single event the magnitude could be similar to the December 2004 earthquake.

Keywords: earthquake stress interactions; seismicity and tectonics; subduction zones; earthquake forecasting and prediction; accelerating moment release

1. Introduction

The earthquake that resulted from slip along about 1600 km of the Sumatra–Andaman subduction system on 26 December 2004 has focused attention on the tsunami danger posed by such massive submarine events [1–4]. Although it was known that events along the Sumatra–Java subduction zone could generate tidal waves, such a massive earthquake was not anticipated since the relative paucity of large events along the arc [e.g. 5,6] led to the conclusion that substantial parts of the arc were uncoupled (aseismic) [7,8] (Fig. 1). Prior to the recent events, known

* Corresponding author.
E-mail address: king@ipgp.jussieu.fr (G. King).

0012-821X/$ - see front matter © 2006 Elsevier B.V. All rights reserved.
doi:10.1016/j.epsl.2006.01.058

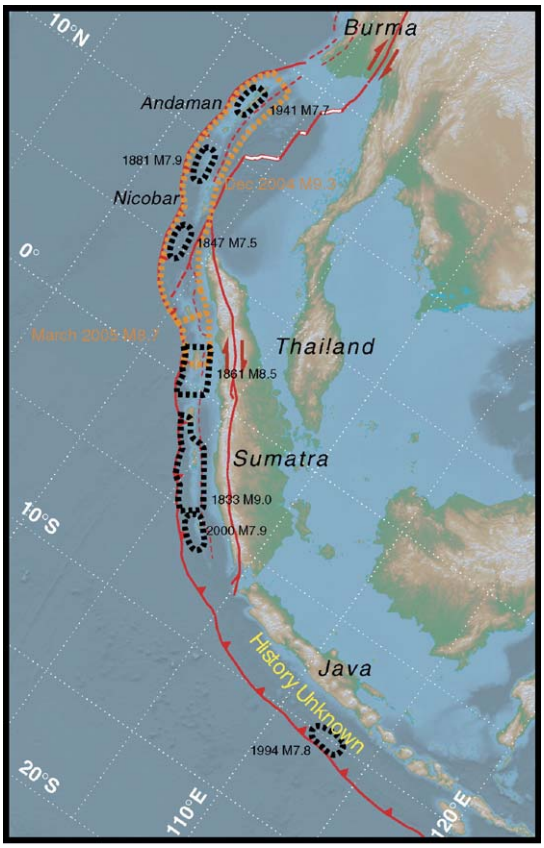

Fig. 1. Large earthquakes (>*M* 7.5) along the Sumatra–Java arc. Estimated rupture regions for historical events are shown in black and the rupture regions for the 26 December 2004 and 28 March 2005 are shown in orange.

historical earthquakes had released little of the slip that had accumulated along the arc in the preceding 2–300 yr. In retrospect, it seems that the historical record was too short to characterize the behavior of the arc [8].

Examining space–time patterns of regional seismicity is increasingly being used as the basis for assessing seismic hazard. In regions where good historical information is available, and taking Eastern Turkey and the Aegean as an example, it has been shown that the concept of seismic gaps can identify faults likely to host substantial events over the coming years or decades [9–11]. The reliability of this approach rests on the assumption that earthquakes repeat regularly, an assumption that many workers regard as unreliable [e.g. 12–14]. The identification of seismic gaps has been complemented in such areas by studies of earthquake stress interactions [e.g. 15,16]. As a result of tertiary creep, the abrupt change of stress due to an earthquake enhances the probability of events over time periods of years in the regions where Coulomb-stress has been increased [17]. This has been quantified using rate and state friction to estimate earthquake probabilities for the period shortly following large events [e.g. 10,18–20]. However, because these studies involve the calculation of stress changes rather than absolute stress, they are of limited use unless a reliable recurrence time can be used to estimate where the region lies in its seismic cycle.

In this paper, we discuss a technique that allows proximity to failure to be assessed without knowledge of the seismic history of the region. The approach is to examine seismic activity in the region that must become loaded prior to an event. Numerous studies have suggested that seismic activity increases over a wide region around a future epicenter, an effect that has been labeled Accelerated Moment Release (AMR). Many explanations for these observations have been offered [21–24] but none established a clear relation between the fault that would fail and the evolving stress field. For events in California however, it has been shown that the increase in activity is found in the regions where stress must accumulate before motion on the future fault can occur and that these can be identified *after* the earthquake has occurred [25,26]. They also propose that AMR can be identified *before* an earthquake if geological data allows the parameters of a possible future event to be identified before it happens. Here, we apply this Stress Accumulation Model [27] to the Sumatra–Java arc and demonstrate that the slip regions of both the 26 December 2004 and the 28 March 2005 events showed clear evidence that they were approaching failure prior to the two events. We further show that the regions of highest slip in the two events correspond to the sections of the arc that exhibited the most pronounced AMR. In contrast, the section of the subduction zone where the 1833 earthquake occurred shows no reliable evidence of accelerating activity at present. However, a region of accelerating seismicity associated with a 750 km stretch of the mapped plate boundary along southeastern Sumatra and western Java suggests that this region may be approaching failure.

2. The stress accumulation model

The mechanical processes of the stress accumulation model (SAM) are discussed in detail by King and Bowman [27]. They describe a complete seismic cycle for an isolated sticking patch on an otherwise creeping strike-slip fault. The model allows synthetic seismic catalogues to be generated that are closely comparable to those observed. An idealized representation of the evolution of stress and seismicity for the last 10% of the earthquake cycle is shown in Fig. 2. This is similar to the

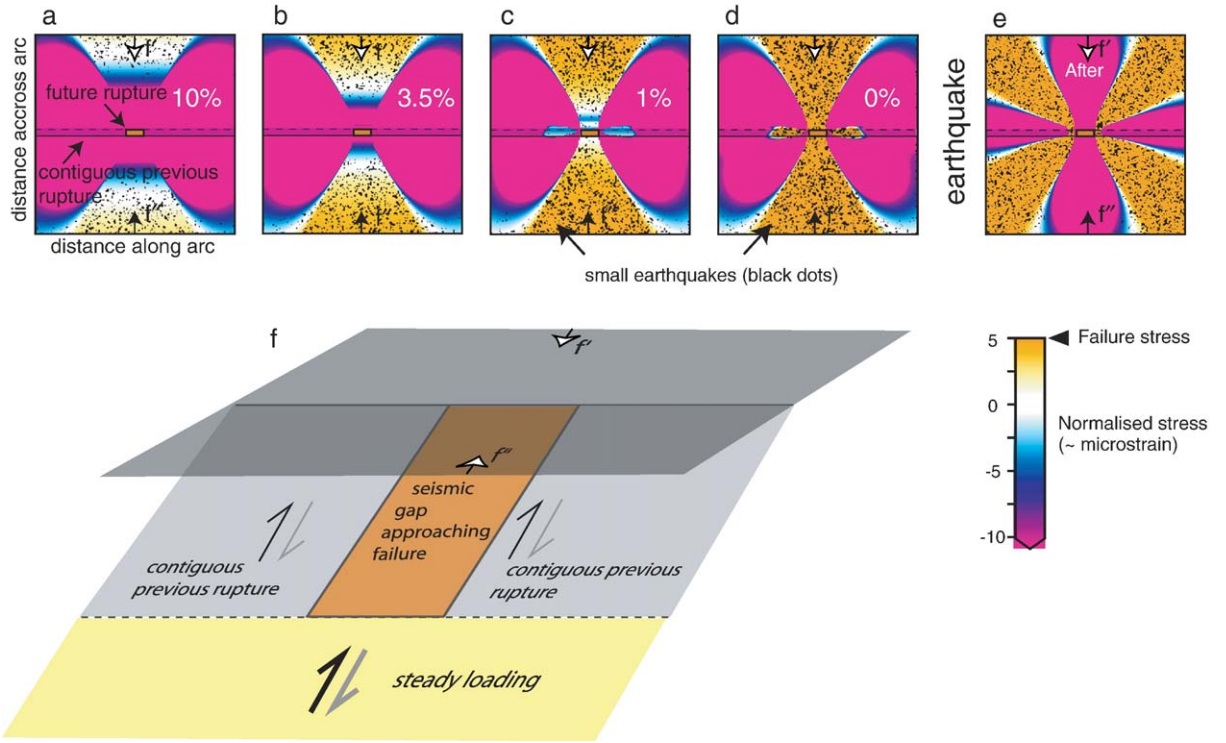

Fig. 2. The evolution of stress and seismicity for the last 10% of the earthquake cycle for a reverse fault. The fault geometry (not to scale) is shown in (f). The faults adjacent to the impending earthquake are considered to be early in their seismic cycle and are locked, while the creeping fault at depth increases in slip from 90% to 100% of the slip required to bring the fault in the seismic gap to failure. Since only slip on the fault at depth increases below a locking depth until the earthquake occurs, this model is identical to those used to model geodetic data. The values used for the model are 7.5 m slip for the adjacent faults, and the slip on the creeping fault below the seismogenic zone increases from 9 to 10 m. (a), (b), (c) and (d) represent the last 10%, 3.5%, 1% and 0% of the seismic cycle. It can be seen that during the last 10% of the cycle, activity (represented by small black dots) rapidly approaches the future epicentre. Following the earthquake the lobe patterns change and the black dots represent aftershocks. The mask to provide the inheritance stress (see [27]) and the colour range are chosen so that failure stress reaches the future fault when deep slip reaches 10 m. The colour bar shows normalized stress. The depth of the seismogenic zone is taken to be 15 km (locking depth) and the length of the fault is 30 km. To produce the artificial earthquakes, random stress variations (referred to as "noise" in [27]) are added to the evolving stress level calculated for realistic earthquake parameters as described above. For this figure the random variations are exaggerated to make the events easily visible. It has previously been shown that, using realistic random variations, a model like this can create artificial seismic catalogues exhibiting AMR that is similar to real earthquake sequences when analysed by the same methods as real catalogues [27].

model described by King and Bowman [27], but calculated for a reverse fault. The faults adjacent to the impending earthquake are considered to be early in their seismic cycle and are locked. The fault at depth creeps with slip increasing from 90% to 100% of the slip required to bring the fault in the seismic gap to failure. Fig. 2a, b, c and d represents the last 10%, 3.5%, 1% and 0% of the seismic cycle. During the last 10% of the cycle, it can be seen that seismic activity (represented by small black dots) rapidly surrounds the future epicentre. This pattern of activity mimics the so-called "Mogi Doughnut", a halo of precursory activity that is sometimes observed around subduction zone earthquakes [28]. Following the earthquake, the stress pattern changes and the location of the seismicity switches to the aftershock lobes. King and Bowman [27] show that realistic values of earthquake stress drops and stress field inhomogeneities can produce artificial catalogues with AMR similar to those observed.

The SAM method [25,26] defines the region where stress must accumulate and pre-event seismicity must occur during the last part of the earthquake cycle. The technique is the same as that used to calculate post-earthquake Coulomb-stress [10,16], but the fault is slipped with the opposite sense (the "backslip" model first described by Savage [29]) to identify the form of the stress field before the earthquake. The form of the stress field is the same for half-space and plate calculations, only the decay with distance is changed [30]. In common with most other Coulomb-stress change studies a half-space calculation is adopted. Fig. 3 shows the method applied to the segment of the

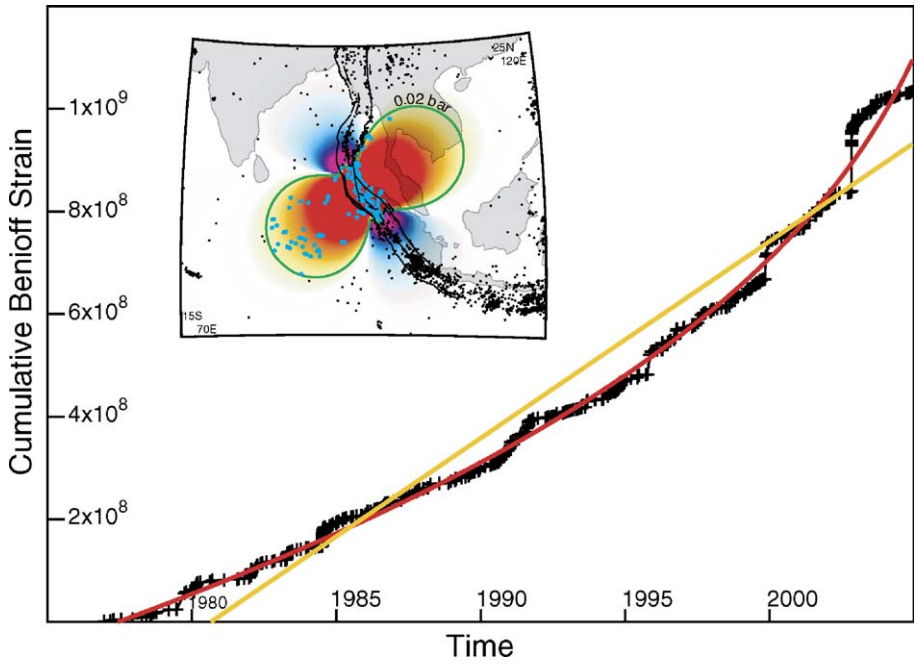

Fig. 3. Accelerating moment release (AMR) for the great Sumatra earthquake of December (12/26/2004). The cumulative Benioff Strain and the time (in years) are respectively the *y*-axis and *x*-axis. The power law fit (red curve) and the line fit (yellow line) used for the calculation of the *c*-value are shown. The *c*-value is 0.28, which corresponds to a 2% probability that the acceleration could occur randomly. The pre-stress field calculated by the backslip earthquake method for the high slip part of the 26 December 2004 event is shown in the inset. The red contour (0.02 bars) outlines the area of events that provides the best *c*-value. Other contours also result in AMR; the one displayed is the optimum. The fault used corresponds to segments 5, 6, and 7 in Table 1. It has a dip of 11°, a down-dip width of 200 km and each segment is pure dip-slip.

subduction zone that experienced the largest and most rapid slip in the 26 December 2004 earthquake. The inset shows the surface projection of the fault as a black line. The outlined region corresponds to the 0.02 bar Coulomb-pre-stress contour for the fault parameters given in the figure caption. The choice of this value is discussed in the next section and in earlier papers [25,26,31], where it is pointed out that the form and not the absolute value of stress is of importance to identify the region that must be loaded prior to an earthquake. The earthquakes (shown by black dots) within this contour demonstrate AMR. The AMR shown in the figure is first identifiable in 1977 with activity steadily increasing until immediately prior to the December earthquake. It should be noted that the increase in activity results not from a few larger events near the end of the period but an overall increase of activity. This provides some support for the view that the AMR is a consequence of a general increase of activity (i.e. an increase of *a*-value and not a change of *b*-value in the Gutenburg–Richter relation) [30,31]. In this example the backslip earthquake model location and parameters are defined by the reported parameters of the event [1].

To examine AMR along the whole arc we divide it into segments. The quality of earthquake catalogues in the Sumatra–Java region places a practical constraint on the size of the segments. In California, where catalogues are complete down to a magnitude of 3.5, it is possible to retrospectively demonstrate AMR before events for $M=6.5$ events whose rupture parameters have been established [25,26]. However, catalogues in the Sumatra–Java region are not homogeneous below magnitude 4.5, so that it is unreasonable to expect to find AMR even for known events smaller than $M\sim7.5$ (fault length ~150 km). With this constraint in mind, the subduction zone is divided into segments ~250 km long to search for AMR before future events. This segmentation length means that only future events significantly greater than $M=8.0$ will be detected.

3. Quantification of accelerating moment release (AMR)

A number of studies have suggested that AMR can be modeled by fitting a simple power law time-to-failure equation of the form

$$\varepsilon(t) = A + B(t_f - t)^m \quad (1)$$

where t_f is the time of the large event, B is negative and m is usually about 0.3. A is the value of $\varepsilon(t)$ when $t=t_f$

[32,33]. The cumulative Benioff strain at time t is defined as

$$\varepsilon(t) = \sum_{i=1}^{N(t)} E_i(t)^{1/2} \quad (2)$$

where E_i is the energy of the ith event and $N(t)$ is the number of events at time t. To quantify the AMR, we use the c-value [22] defined to be the ratio between the root mean square of the power law time-to-failure fit (Eq. (1)) and the root mean square of a linear fit to the cumulative energy of events. If the c-value tends to zero, a power law best approximates the curve and AMR is observed. If the c-value tends to unity then no AMR is seen. For a specified source (known or proposed) the program Nutcracker (http://geology.fullerton.edu/dbowman/downloads/NutcrackerX.1.zip) automatically searches for low c-values within a range of Coulomb-stress contours and a range of catalogue start-times. From this matrix, start-times and stress levels can be identified that exhibit AMR, together with sensitivity of the AMR to parameter changes.

The stress levels identified in this procedure are used to define the shape of the stressed region (see Fig. 3). For any given azimuth, the extent of the pre-stress region depends on the fault slip. If known fault slip is used following an earthquake, the stress contours correspond to stress change at the time of the event. Where events have not yet happened, a nominal fault slip is selected and the values of the stress contours should be taken only as a rough guide. Clearly variations in modulus such as that between ocean and continental crust will modify stress contours, but such an effect is minor compared to other limitations of the approach addressed in the discussion.

Since the algorithm automatically seeks regions of low c-value, some degree of AMR will nearly always be found. To determine if the acceleration is due to a 'real' physical process or is merely a result of random clustering, we have used the Monte Carlo technique to examine the likelihood of AMR in random catalogues. Because any AMR found in these random catalogues cannot be due to a physical process, they provide a way of estimating the reliability of any give AMR sequence [34] (further information can be found in the Appendix). For the example in Fig. 3 the technique suggests that there is less than a 2% possibility that the observed AMR is due to random processes. In the study of the Sumatra–Java arc that follows, the reliability of the observed AMR is assessed by *direct observation*, examining the *start-time versus stress matrix* and the c-value (see Appendix). The *total time* over which the acceleration is observed is also an important guide. The length of the AMR is related to the length of the seismic cycle [27] and consequently a short total time suggests that the AMR is incomplete and the region not yet fully re-stressed. This is consistent with such regions rupturing only as a consequence of propagation of slip from more stressed regions (as discussed below). However, an AMR with a short total time also contains fewer events and is of less statistical significance than a longer time period.

4. Accelerating moment release along the Sumatra–Java arc

The method outlined above has been applied along the length of the Sumatra–Java Arc (Fig. 4). The mechanisms are assumed to be pure reverse faulting

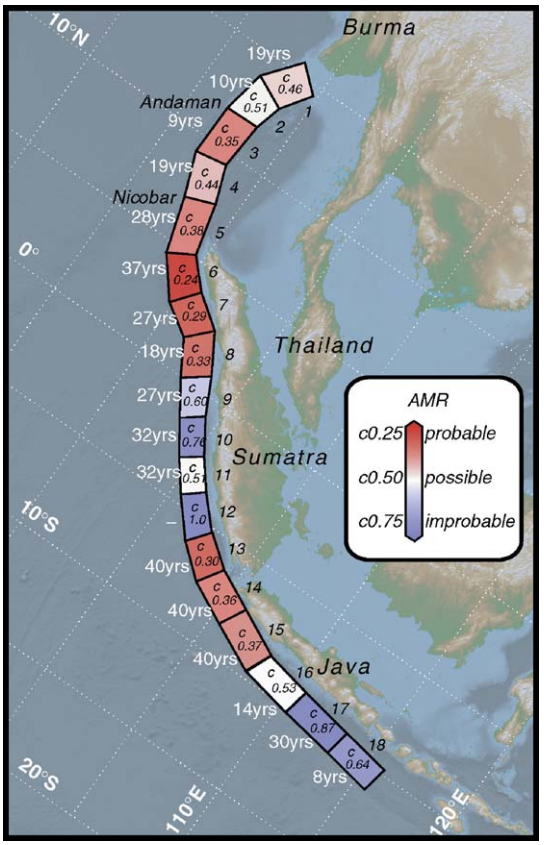

Fig. 4. AMR for the Sumatra–Java arc. For each segment the c-value is indicated and shaded in accordance with the colour bar in the inset. Beside each segment the length of time over which AMR is identified is indicated in years. The segments are numbered and the corresponding c-values, duration of AMR and probability that the AMR is non-random is shown in Table 1. The co-ordinates of the ends of the segments are also provided. Each segment has a dip of 11°, a width of 200 km and is pure dip-slip with a nominal displacement of 20 m.

with a dip of 11° and a width of 200 km. The regional stress for the Coulomb calculation [16] is chosen so that the greatest compressive stress is approximately perpendicular to the arc for each segment. The segments are shaded according to their *c*-value. The total time over which AMR can be identified is indicated beside each segment. The segments are numbered and the corresponding *c*-values, total time and the probability that the AMR is non-random (*reliability*, see Appendix) are shown in Table 1.

Fig. 5 shows the slip distributions for the 26 December 2004 and the 28 March 2005 events [adapted from 1], which can be compared to the AMR for the event. The maximum slip in the December 2004 event corresponds to three segments 5, 6, and 7, while the maximum slip in the March 2004 event is in segment 8. Each segment individually had low *c*-values corresponding to less than 4% probability that they resulted from random processes. Segments 1 to 4 also exhibited AMR before the 26 December event, but with lower significance. In each of these cases, the time period over which AMR is observed is also relatively short. The higher *c*-value, and shorter time period, together with an inspection of the plots of Benioff strain (see discussion in the Appendix), suggests that the AMR for these parts of the fault are less convincing. Nonetheless, the AMR is consistent with segments 1 to 4 being loaded, albeit less dramatically than segments 5, 6, and 7. This is consistent with the lower slip on the northern segments during the earthquake. The 26 December earthquake initiated where the AMR was clearest and where the subsequent slip was greatest. The 28 March event also initiated where the AMR was clear and propagated to segment 9 where AMR is less clear. The evidence for AMR for segment 10 is almost absent and there is little evidence of AMR for segment 11 and none for segment 12. Further south, for segments 13,14 and 15 significant AMR is observed with values similar the zones that experienced the highest slip in December 2004 and March 2005. Segments 16 to 18 have no significant AMR but the results may be contaminated by stress systems and seismicity associated with the Banda and Philippine arc.

5. Discussion

The cartoon evolution shown in Fig. 2 shows a rapid evolution with seismicity steadily approaching the future epicentre during the last 10% of the earthquake cycle and is calculated in a similar way to that used by King and Bowman [27] (see the figure caption). For real situations, effects that are not considered for the simple model can intervene. The model supposes that the earthquake cycle consists of one simple loading system, where the only elements are creep at depth and the seismic motion of adjacent faults. At the end of the

Table 1
Segment characteristics

Segment	Segment start		Segment finish		*c*-value	Reliability	Total time
	Lat°	Long°	Lat°	Long°		(%)	(yr)
1 (Slow rupture associated with the 26 December 2004 event)	93.48	15.58	92.03	13.85	0.46	84	19
2 (Slow rupture associated with the 26 December 2004 event)	92.04	13.85	91.60	11.69	0.51	76	10
3 (Slow rupture associated 26 December 2004 event)	91.60	11.69	91.53	9.17	0.35	98	9
4 (Slow rupture associated 26 December 2004 event)	91.53	9.17	92.37	7.01	0.44	88	19
5 (26 December 2004 event)	92.37	7.01	92.86	4.28	0.38	96	28
6 (26 December 2004 event)	92.86	4.28	94.55	2.92	0.24	99	37
7 (26 December 2004 event)	95.55	2.92	96.48	1.33	0.29	98	27
8 (28 December 2004 event)	96.48	1.33	97.30	−0.13	0.33	97	18
9 (1861 event)	97.30	−0.13	98.26	−1.59	0.60	50	27
10 (1833 event)	98.26	−1.59	99.36	−3.19	0.76	23	32
11 (1833 event)	99.36	−3.19	100.53	−4.99	0.51	70	32
12 (1833 event)	100.53	−4.99	101.97	−6.63	1.0	0	–
13 (History unknown)	101.98	−6.63	103.76	−7.93	0.30	98	40
14 (History unknown)	103.76	−7.93	105.68	−8.74	0.36	97	40
15 (History unknown)	105.68	−8.74	108.28	−9.86	0.37	96	40
16 (History unknown)	108.28	−9.86	111.18	−10.21	0.53	76	14
17 (History unknown)	111.19	−10.21	114.81	−10.61	0.87	20	30
18 (History unknown)	114.81	−10.61	118.38	−10.56	0.64	60	8

The fault segments all dip at 11°, a width of 200 km and are pure dip-slip. The regional stress field is chosen accordingly (see text). Since AMR is a far field effect it is not very sensitive to the fault parameters (see Appendix). The reliability and a long total time suggest that the AMR indicates that the segment is loaded. A long total time has no significance if the reliability is low.

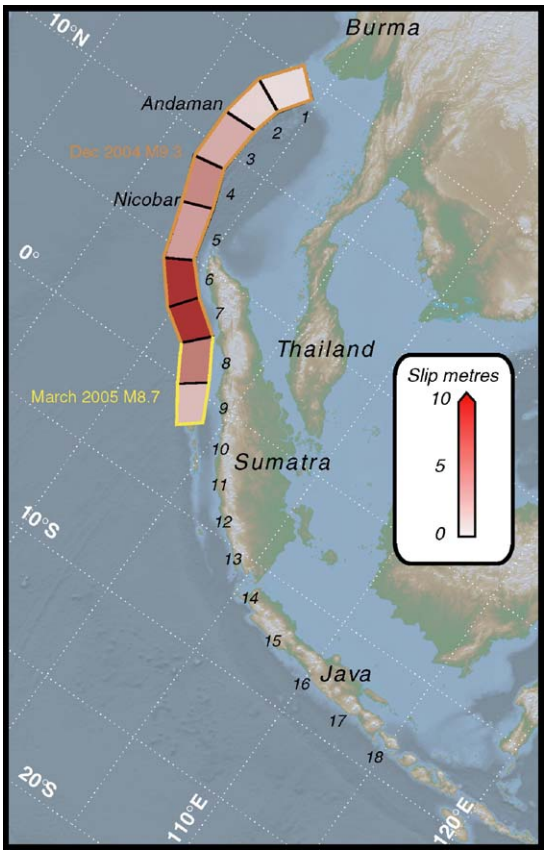

Fig. 5. Simplified slip distribution for the ruptures of the 26 December 2004 and 28 March 2005 earthquakes (modified from [1]). The displacements are shown in metres. Red shading also represents slip with a range from 0 m — white to 10 m — red.

cycle, the stress conditions are identical to those at the beginning; the assumptions of a simple elastic rebound model. Elastic rebound concerns only horizontal stresses and displacements, however some permanent deformation (topography) is created at the end of the earthquake cycle for a dip-slip fault [35–37]. The flexure, uplift, and subsidence associated with dip-slip earthquakes are associated with their own seismicity, which perturbs that expected for an idealized earthquake cycle. In more general terms, complex fault geometries result in the superposition of the stress fields and associated seismicity of multiple faults at different stages in their loading cycles. It is important to appreciate that the strain energy involved in these processes is very small and localized near to the earthquake epicentral region. The strain energy stored prior to, and then released in the main shock, is much greater. For Sumatra geodetic displacements of 1 or 2 cm occurred in India and Indonesia indicating the release of stress in a region larger than those in which we identify AMR.

Other major faults or plate boundaries can be associated with stress fields that are not responsible for the future earthquake. For example, the loading of the strike-slip fault behind the arc and the associated seismicity involves stress fields that cannot result in the observed dip-slip motion. Since at present such seismicity cannot be separated, events associated with loading of the strike-slip fault could be a source of error in the AMR plot for reverse faulting events. A similar situation occurs for western Java where the Banda and Philippine arcs and associated seismicity are sufficiently close that they overlap with regions that must be stressed prior to an eastern Java event.

While these sources of error reduce our ability to identify AMR they also offer future approaches to improving signal to noise ratios. The most straightforward would be to use only precursory events with identified focal mechanisms. Unfortunately, at present there are few parts of the world where seismic catalogues both include mechanisms and are homogeneous. The stress field prior to an event also varies with depth in a manner that can readily be calculated to improve the results. Unfortunately, most earthquake catalogues have poor depth resolution, rendering such an approach ineffective. While the limitations of existing catalogues must be accepted, future improvements may allow much improved AMR studies.

Prior to the work of King and Bowman [27], it was assumed that AMR was correctly modeled by Eq. (1), based on the assumption that the events prior to the earthquake were part of either a failure process or a process analogous to a phase transition. The stress accumulation model [27], in which creep at depth progressively fills a stress shadow, requires that events are a symptom of the loading process and are not a part of the failure leading to the main event. There is consequently no reason to suppose that the main event should occur at the asymptote of the failure function. The use of a power law time-to-failure function (Eq. (1)) is used in this study since the filling of the stress shadow cannot be reduced to a simple analytic expression. In the future it may be possible to generate more appropriate empirical expressions for the AMR. However, in the absence of a clear alternative, Eq. (1) is retained on the understanding that the asymptote has no physical significance. It follows that since we do not know at present how much acceleration must be observed before an earthquake occurs, a clear time prediction is not possible.

The results presented above suggest that part of the southern Sumatra and western Java arc is now subject to similar loading conditions to those that prevailed prior to

the Sumatra earthquakes of 26 December 2004 and 28 March 2005. The data presented is very suggestive, but would be more certain if we had more examples of AMR before large subduction earthquakes. Unfortunately although very large events have occurred (e.g. Chile 1960, Alaska 1965) the NEIC catalogue is not long enough to provide the clear accelerations that span 10s of years. Where acceleration is identified over shorter time spans, it is more equivocal.

In the absence of many examples it is uncertain when the southern Sumatra and western Java arc might fail. Models suggest that the most pronounced AMR is within the last 10% of the earthquake cycle (which is perhaps between 200 and 500 yr for the Sumatra–Java subduction system). AMR should therefore be identifiable in the last 20 to 50 yr before the event. Thus, an AMR total time of 40 yr might suggest that the event will occur in the next few years, but this is far from certain.

Various workers have proposed that some subduction systems are coupled and seismic, while some are uncoupled and largely aseismic. This has been explained by mechanical models that invoke parameters including (but not limited to) subduction rate, sediment load, and motion of the trench relative to the mantle as determining the seismic coupling [38–40]. However, the seismic observations on which these models are based cover about 100 yr, which may not be a sufficiently long time period for the characterization of slow subduction systems [40]. For both the Sumatra (north and central) and Cascadia subduction systems, hitherto regarded as uncoupled, geological investigations have already demonstrated that this is incorrect [8,41–43]. It is therefore pertinent to question the implications of AMR in a subduction setting that has previously been considered to be uncoupled, such as southern Sumatra and western Java. Certainly the progressive build-up of stress implied by the stress accumulation model [27] is not consistent with steadily creeping subduction. However, recent observations of transient strain events in subduction settings [e.g. 44] and theoretical models [45] although concerning much smaller scales might suggest that the current period of AMR could be precursory to a non-destructive, slow earthquake.

6. Conclusions

Parts of the Sumatra–Java arc exhibited clear Accelerated Moment Release (AMR) prior to the 26 December 2004 and 28 March 2005 earthquakes. On the basis of a simple loading model of the type widely accepted to explain geodetic observations (Fig. 2 and caption), we propose a model in which the AMR provides evidence that sections of the arc were approaching failure prior to the catastrophic events. The method that we use has the potential to directly estimate absolute stress (relative to failure stress), a significant advance on Coulomb-stress change models [16]. If demonstrated to be robust, an ability to independently identify the latter part of the seismic cycle will enhance seismic gap methods of establishing earthquake risk.

The epicentres of both events occurred where AMR, and hence loading, was greater and propagated into regions where loading was less. To the south of the slip regions of the recent events, the epicentral area of the 1833 earthquake shows no evidence for an impending earthquake. Recent studies of corals suggest that this region is nearing the end of the earthquake cycle [46], but the event could still not be close enough for AMR to be observable yet. However further to the south and east, parts of the Java–Sumatra arc appear to be loaded and may be capable of hosting a devastating earthquake

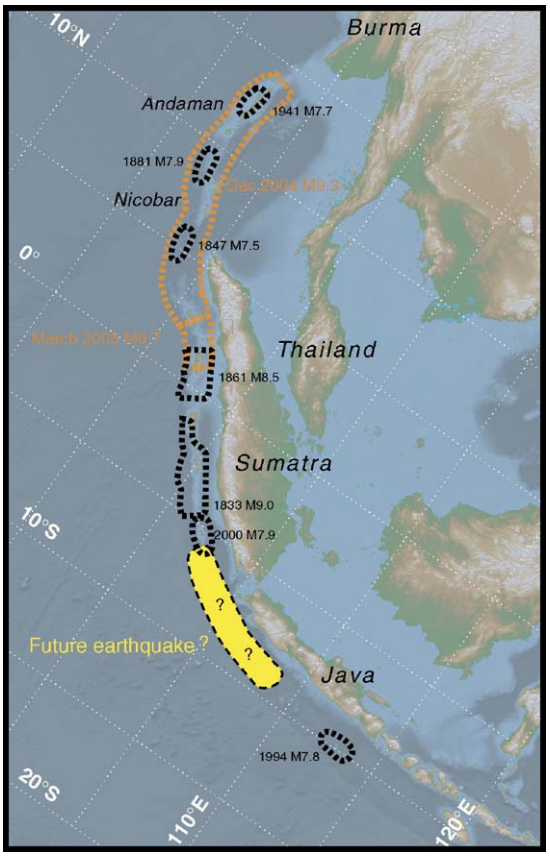

Fig. 6. The region where observed AMR suggests that the subduction system is approaching the end of the seismic cycle (yellow).

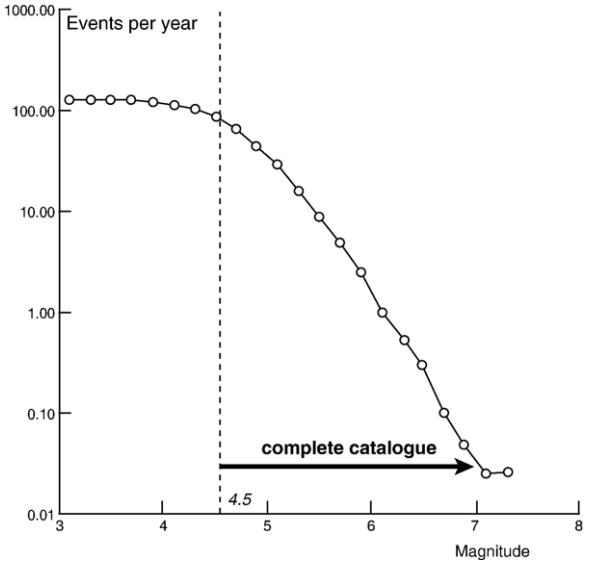

Fig. A1. The Gutenburg–Richter plot for the data used to calculate AMR along the Sumatra–Java arc. The catalogue is complete above M 4.5. Subsets of the catalogue in time and space have also been examined to establish this throughout the region.

(Fig. 6). In the absence of further studies in different regions, a possibility limited by the length of the available seismic catalogues, we cannot be certain that our results truly indicate an imminent earthquake danger for southeastern Sumatra and western Java. However, our conclusions rest on a simple physical/mechanical model. Bearing in mind the consequences, such an event should be taken seriously.

Acknowledgements

The authors thank Paul Tapponnier and Jim Rice for helpful suggestions and critical comments. Roger Bilham provided a most helpful review that has substantially improved the manuscript. This research was supported by the Southern California Earthquake Center and NSF grant EAR-0510196. SCEC is funded by NSF Cooperative Agreement EAR-0106924 and USGS Cooperative Agreement 02HQAG0008. This paper is IPGP Contribution number 2111, INSU contribution number 390 and SCEC contribution number 995.

Appendix A

A.1. Seismic data

The seismicity catalogues required for examining AMR must be homogeneous. Except for a few places, such as California, this can only be satisfied using the global catalogue based on the NEIC (ANSS) data set. The catalogue used here was taken from the Advanced National Seismic System (ANSS) Worldwide Earthquake Catalog, accessible from the Northern California Earthquake Data Center (http://quake.geo.berkeley.edu/anss), and extended from 01/01/1965 to 24/12/04. The minimum magnitude used was 4.5. This was chosen by examining the frequency–magnitude statistics of the catalogue to define the minimum magnitude where a stable Gutenburg–Richter relation is observed [47] (e.g. Fig. A1). Because progressive improvements in the global seismic network have resulted in a progressive lowering of the detection threshold of small events, this step is necessary to remove apparent AMR caused by changing catalogue completeness.

Only events with depths from the surface to 40 km were used. This is chosen to include those events with depths fixed at 33 km. The stress calculation was carried out for a depth of 8 km. Since the AMR is associated with seismicity distant from the future epicentre this is sufficiently accurate for the range of earthquake depths considered. Deeper events, in particular those associated with the lower part of the lithosphere and the subducting slab, may exhibit changes associated with the build-up of load on the future fault [48–51] but would require a three dimensional stress model and a more complicated search of the stress–time grid. This will be investigated in future work.

A.2. c-value and statistics

A measure of the reliability of the acceleration in a certain spatiotemporal area in a catalogue of seismicity is carried out by calculating the c-value, which is the ratio between the root mean square of a power law fit

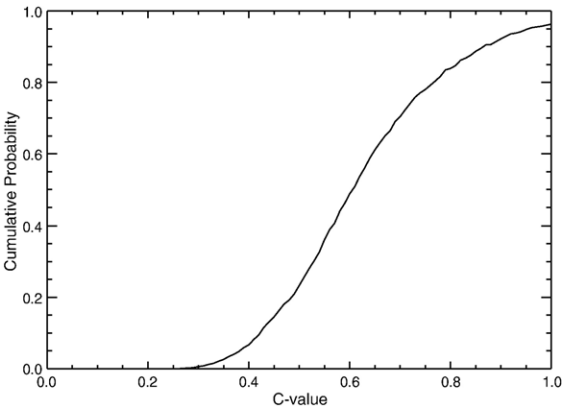

Fig. A2. The probability of different c-values occurring in a random catalogues.

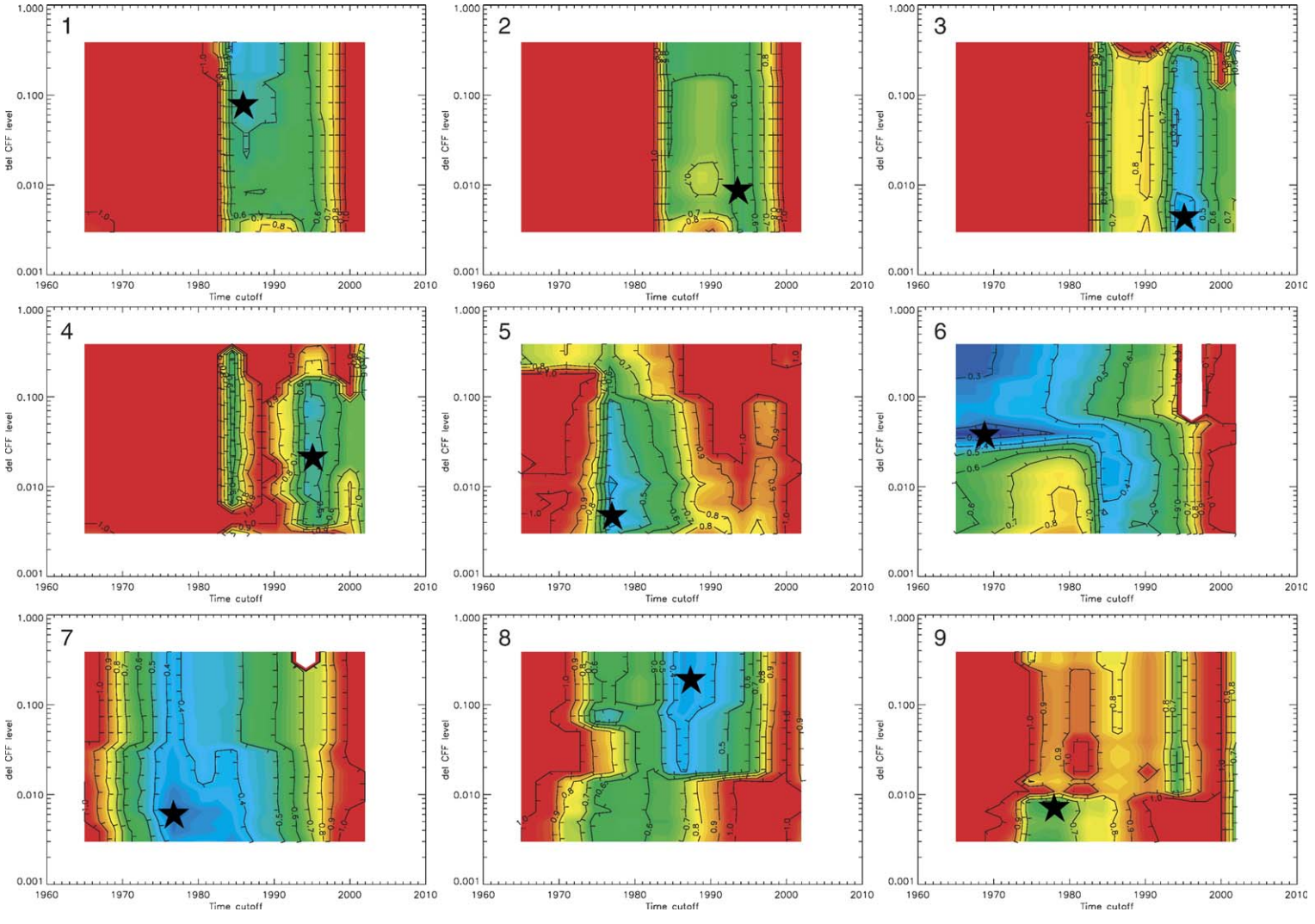

Fig. A3. Start-time versus stress grids for the correspondingly numbered segments shown in the figures in the main text.

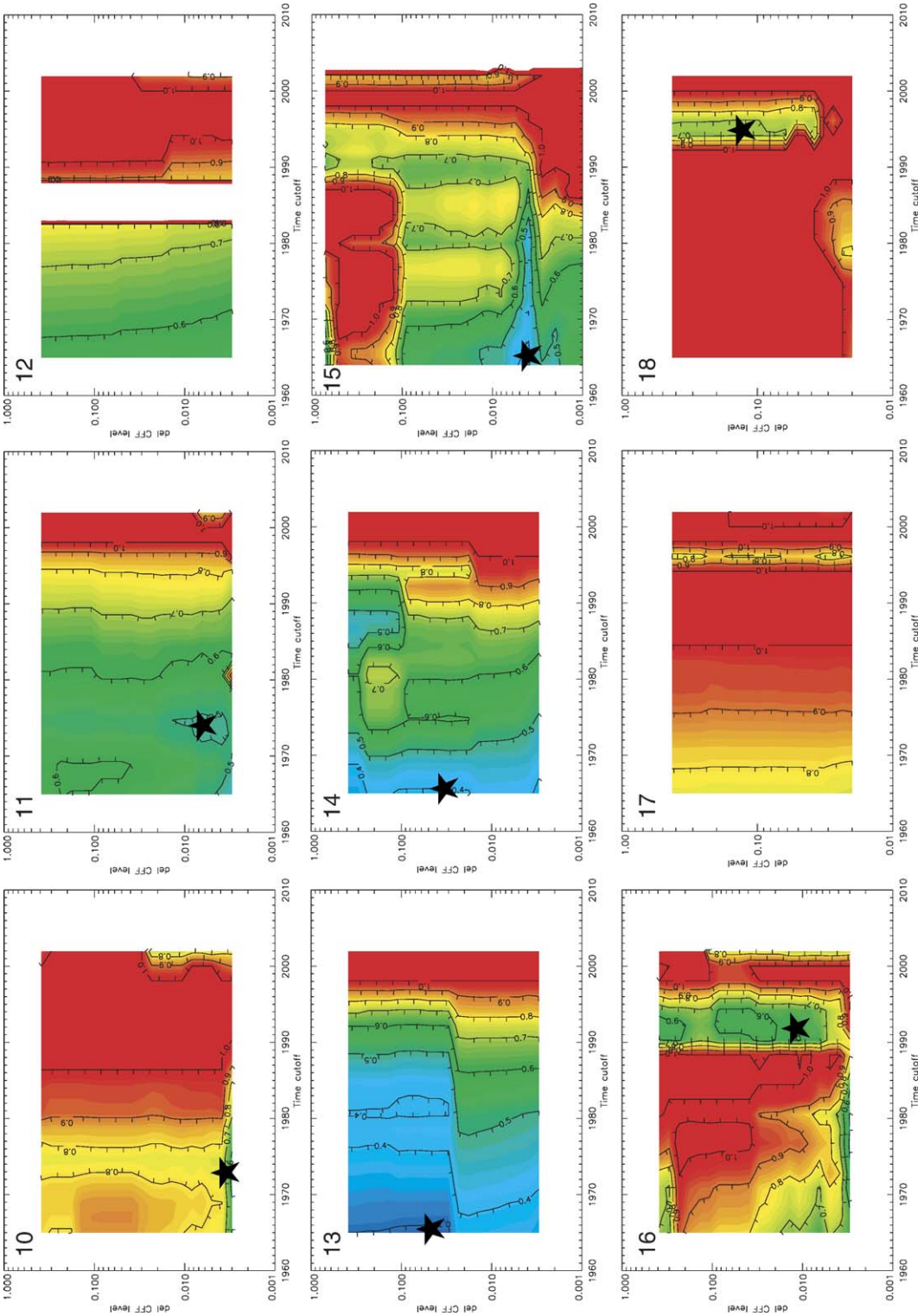

Fig. A3 (*continued*).

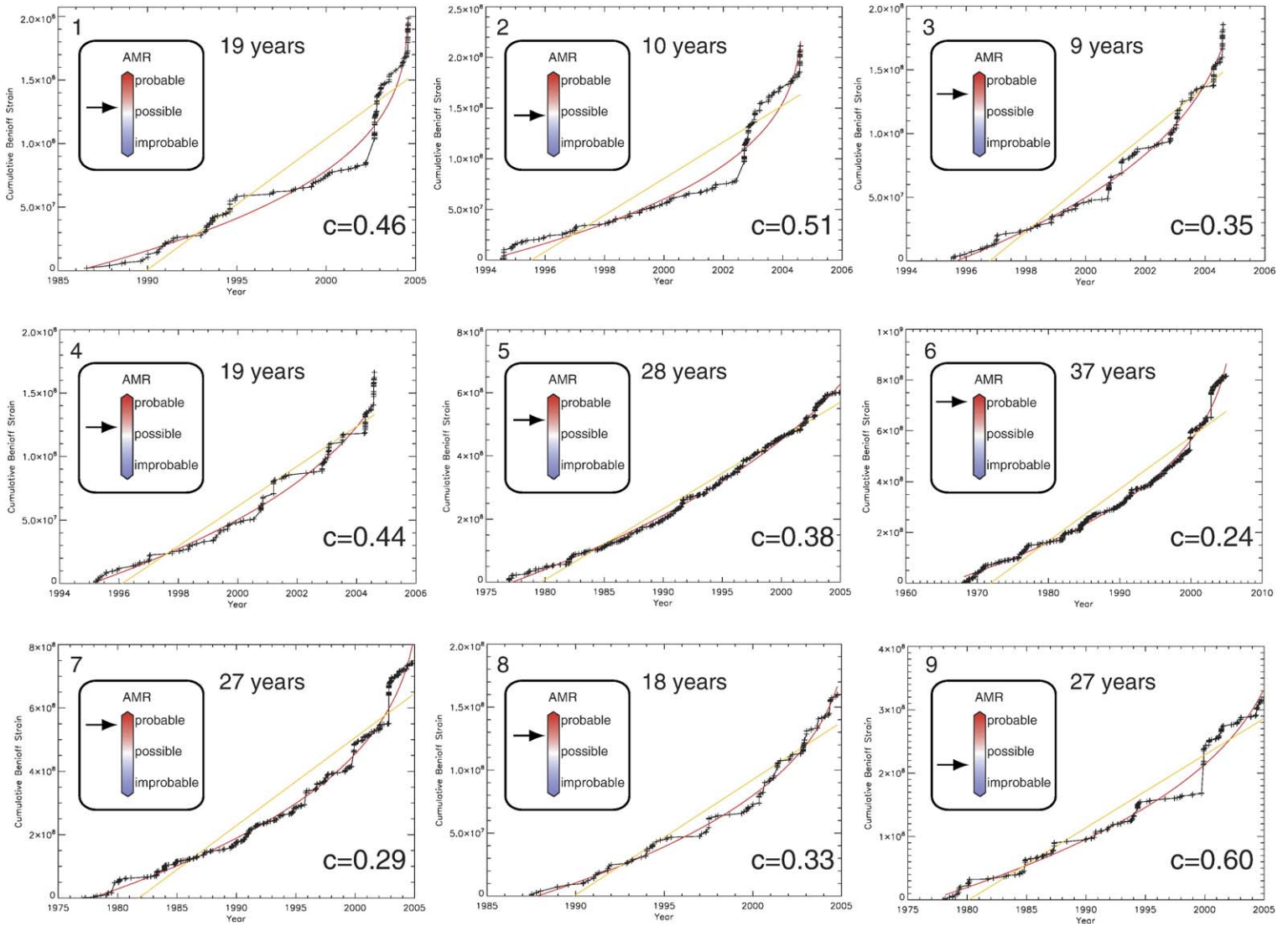

Fig. A4. The AMR plots chosen to be representative for the correspondingly numbered segments shown in the figures in the main text. Information for each segment is provided in Table 1 of the main text. The insets indicate the reliability of each plot. See the main text.

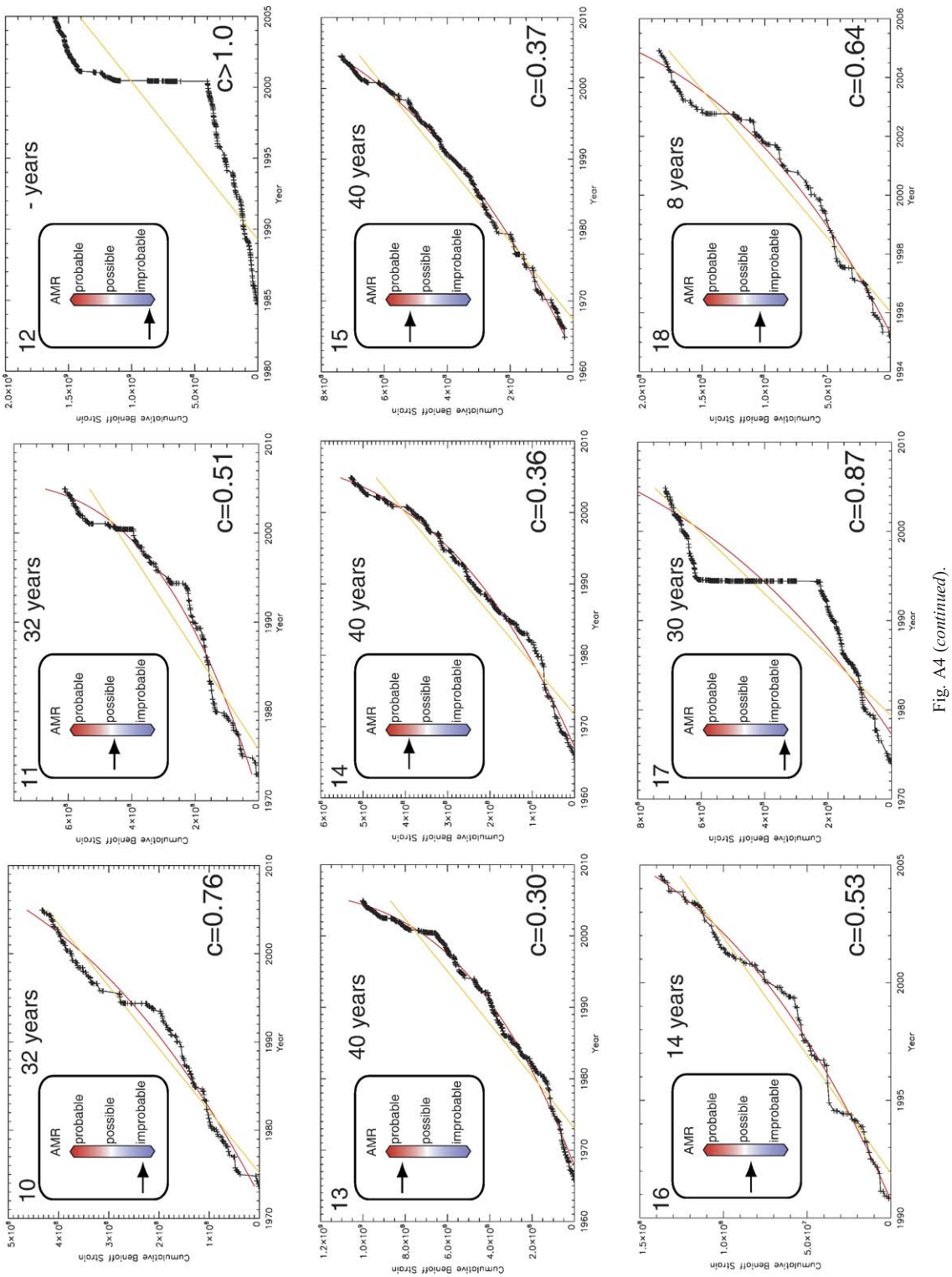

Fig. A4 (*continued*).

and the root mean square of a linear fit [22]. If the *c*-value tends to zero, the curve is best approximated by a power law and if the *c*-value tends to the unity, the curve can be best approximated by a straight line. Because the method searches for acceleration, data sets may exhibit AMR that has no physical origin. To help determine whether an acceleration is likely to be "real" we have examined random catalogues of synthetic seismicity.

The Monte Carlo method is used to test the probability that AMR can be found due to random patterns in seismicity (the "false-alarm rate"). 1000 catalogues each composed of 500 events placed randomly in space and time are created. Each point is indexed to a magnitude that respects the Gutenburg–Richter law. Energy for each point is calculated using the magnitude-energy scaling law ($E=10^{4.8+1.5*M}$) [52]. This is then used to generate the cumulative Benioff strain curve. When real data is examined, the shape of the spatial region examined depends on the fault mechanism of the earthquake being examined. While there is no obvious reason why shape should affect the results, we test the false-alarm rate for circular, square and triangular patterns.

For each geometrical pattern, the search is done using a spatiotemporal matrix (*c*-value=*f* {pattern, distance to the centre of the pattern, starting time}). In detail, for the circle example, events are localized in a unit square ([0,0;0,1;1,0;1,1]) and the centre of the circle corresponds to the centre of the synthetic catalogue. The calculation of *c*-value is first done by looking at events located in a circle of minimum radius (fixed parameter). For these chosen points, another search is done in time by increasing the value of the starting time of the cumulative energy curve (from 0.00 to 0.90 — fixed parameters). This temporal search is repeated several times for the spatial search from the minimum radius to the maximum radius (from 0.05 to 0.50 — fixed parameters). When the *c*-value is calculated for all increments, the best one is kept (minimum *c*-value). This is repeated for each synthetic catalogue and a distribution of minimum *c*-values is then obtained. The search using other geometrical patterns adopts the same method by systematically changing the size of the geometrical figure. The relation between the probability of occurrence and *c*-value is the same for the three geometries tested, and is shown in Fig. A2.

From the figure it can be concluded that low *c*-values (<0.35) are very unlikely to occur by chance. However, once a *c*-value of 0.6 is reached the probability that it could result from random processes is about 50%. In a separate study, different ways of generating random catalogues have been adopted [34]. These include randomizing the times of real catalogues, using real epicentral distributions and assigning random earthquakes to them, and establishing catalogues that adopt the ETAS method to simulate aftershocks [53,54] For *c*-values of 0.6 the probability that the observed AMR can be a random effect can increase to 55%. However for *c*-values less than 0.35 the probabilities are approximately equal to those in Fig. A2. We consequently conclude that *c*-values less than 0.35 have a high probability of being real and those of 0.6 have little significance. As discussed in the text, a low *c*-value is a necessary condition for determining whether an AMR is real. However, it is not a sufficient condition.

A.3. Results for all segments

The start-time versus stress grid for all of the segments is shown in Fig. A3. The vertical axis shows the Coulomb-stress level and the horizontal axis the time period. For each combination of Coulomb-stress and time range, the plots indicate the *c*-value of the associated AMR plot. Reds indicate high *c*-values and blues low *c*-values. The *c*-values are also contoured. The best *c*-value is provided by choosing a blue region. In each start-time versus stress grid, stars indicate the point chosen for the corresponding AMR plot in Fig. A4. In some cases an apparently low *c*-value can be of little significance. In Fig. A3 for example, the blue regions marked bad for segment 1 result from a search very close to the future fault slip; too few events are included to produce a convincing plot. It is important to appreciate that the reliable low *c*-values for segments 6, 7, 8, 14 and 15 are unambiguous.

References

[1] C.J. Ammon, J. Chen, H.K. Thio, D. Robinson, S. Ni, V. Hjorleifsdottir, H. Kanamori, T. Lay, S. Das, D. Helmberger, G. Ichinose, J. Polet, D. Wald, Rupture process of the 2004 Sumatra–Andaman earthquake, Science 308 (2005) 1133–1139.

[2] R. Bilham, A flying start, then a slow slip, Science 305 (2005) 1126–1127.

[3] T. Lay, H. Kanamori, C.J. Ammon, M. Nettles, S.N. Ward, R. Aster, S.L. Beck, S.L. Bilek, M.R. Brudzinski, R. Butler, H.R. DeShon, G. Ekström, K. Satake, S. Sipkin, The great Sumatra–Andaman earthquake of 26 December 2004, Science 308 (2005) 1127–1133.

[4] J. McCloskey, S.S. Nalbant, S. Steacy, Earthquake risk from co-seismic stress, Nature 434 (2005) 291.

[5] M. Ortiz, R. Bilham, Source area and rupture parameters of the 31 December 1881 M_w=7.9 Car Nicobar earthquake estimated from tsunamis recorded in the Bay of Bengal, J. Geophys. Res. 108 (2003) 2215–2230.

[6] J. Zachariasen, K. Sieh, Submergence and uplift associated with the giant 1833 Sumatran subduction earthquake: evidence from coral microatolls, J. Geophys. Res. 104 (1999) 895–919.
[7] L. Prawirodirdjo, Y. Bock, R. McCaffrey, J. Genrich, E. Calais, C. Stevens, S.S.O. Puntodewo, C. Subarya, J. Rais, P. Zwick, Fauzi, Geodetic observations of interseismic strain segmentation at the Sumatra subduction zone, Geophys. Res. Lett. 24 (1997) 2601–2604.
[8] M. Simoes, J.P. Avouac, R. Cattin, P. Henry, The Sumatra subduction zone: a case for a locked fault zone extending into the mantle, J. Geophys. Res. 109 (2004), doi: 10.1029/2003JB002958.
[9] A. Hubert-Ferrari, A. Barka, E. Jacques, S.S. Nalbant, B. Meyer, R. Armijo, P. Tapponnier, G.C.P. King, Seismic hazard in the Sea of Marmara following the Izmit earthquake, Nature 404 (2000) 269–273.
[10] R.S. Stein, The role of stress transfer in earthquake occurrence, Nature 402 (1999) 605–609.
[11] Y.M.N. Toksoz, A.F. Shakal, A.J. Michael, Space–time migration of earthquakes along the North Anatolian fault zone and seismic gaps, Pure Appl. Geophys. 117 (1979) 1258–1270.
[12] L. Benedetti, R. Finkel, D. Papanastassiou, G. King, R. Armijo, F.J. Ryerson, D. Farber, F. Flerit, Post-glacial slip history of the Sparta fault (Greece) determined by 36Cl cosmogenic dating: evidence for non-periodic earthquakes, Geophys. Res. Let. 10 (2002) 1029–2001.
[13] P.B. Rundle, J.B. Rundle, K.F. Tiampo, J.S. Sa Martins, S. McGinnis, W. Klein, Nonlinear network dynamics of earthquake fault systems, Phys. Rev. Lett. 87 (2001), doi: 10.1103/PhysRevLett.87.148501.
[14] R. Weldon, K.M. Scharer, T. Fumal, G. Biasi, Wrightwood and the earthquake cycle: what a long recurrence tells us about how faults work, GSA Today 14 (2004) 4–10.
[15] S. Nalbant, A. Hubert, G.C.P. King, Stress coupling in North West Turkey and the North Aegean, J. Geophys. Res. 103 (1998) 24,469–24,486.
[16] G.C.P. King, M. Cocco, Fault interaction by elastic stress changes: new clues from earthquake sequences, Adv. Geophys. 44 (2000) 1–38.
[17] C.H. Scholz, The Mechanics of Earthquakes and Faulting, Cambridge Univ. Press, New York, 1990, 439 pp.
[18] C.H. Scholz, Earthquakes and friction laws, Nature 391 (1998) 37–42.
[19] A.M. Freed, Earthquake triggering by static, dynamic and postseismic stress transfer, Annu. Rev. Earth Planet. Sci. 33 (2005) 335–367.
[20] M.C. Gerstenberger, S. Wiemer, L.M. Jones, P.A. Reasenberg, Real-time forecasts of tomorrow's earthquakes in California, Nature 435 (2005) 328–331.
[21] D. Sornette, C.G. Sammis, Complex critical exponents from renormalization group theory of earthquakes: implications for earthquake predictions, J. Phys. I 5 (1995) 607–619.
[22] D.D. Bowman, G. Ouillon, C.G. Sammis, A. Sornette, D. Sornette, An observational test of the critical earthquake concept, J. Geophys. Res. 103 (1998) 24,359–24,372.
[23] J.R. Grasso, D. Sornette, Testing self-organized criticality by induced seismicity, J. Geophys. Res. 103 (1998) 29,965–29,987.
[24] C.G. Sammis, S. Smith, Seismic cycles and the evolution of stress correlation in cellular automaton models of finite fault networks, Pure Appl. Geophys. 155 (1999) 307–334.
[25] D.D. Bowman, G.C.P. King, Accelerating seismicity and stress accumulation before large earthquakes, Geophys. Res. Lett. 28 (2001) 4039–4042.
[26] D.D. Bowman, G.C.P. King, Seismicity changes before large earthquakes, C. R. Acad. Sci. Paris 333 (2001) 591–599.
[27] G.C.P. King, D.D. Bowman, The evolution of regional seismicity between large earthquakes, J. Geophys. Res. 108 (2003) 2096–2111.
[28] K. Mogi, Some features of recent seismic activity in and near Japan: 2. Activity before and after great earthquakes, Bull. Earthq. Res. Inst. (Tokyo) 47 (1969) 395–417.
[29] J.C. Savage, A dislocation model of strain accumulation and release at a subduction zone, J. Geophys. Res. 105 (1983) 3095–3102.
[30] R.S. Stein, G.C.P. King, J. Lin, Stress triggering of the 1994 $M=6.7$ Northridge, California, Earthquake by its Predecessors, Science 265 (1994) 1432–1435.
[31] C.G. Sammis, D.D. Bowman, G.C.P. King, Anomalous seismicity and accelerating moment release preceding the 2001 and 2002 earthquakes in northern Baja California, Mexico, Pure Appl. Geophys. 161 (2004) 2369–2378.
[32] D.D. Bowman, C.G. Sammis, Intermittent criticality and the Gutenberg–Richter distribution, Pure Appl. Geophys. 104 (2004) 1945–1956.
[33] C.G. Bufe, D.J. Varnes, Predictive modeling of the seismic cycle of the greater San Fransisco Bay region, J. Geophys. Res. 98 (1993) 9871–9883.
[34] N. Ikeda, Testing the false alarm rate of accelerating moment release before large earthquakes, M.S. Thesis, California State university, Fullerton, 2004.
[35] G.C.P. King, R. Stein, J. Rundle, The growth of geological structures by repeated earthquakes: 1. Conceptual framework, J. Geophys. Res. 93 (B11) (1988) 13307–13318.
[36] R.S. Stein, G.C.P. King, J. Rundle, The growth of geological structures by repeated earthquakes: 2, field examples of continental dip-slip faults, J. Geophys. Res. 93 (B11) (1988) 13319–13331.
[37] R. Cattin, J.P. Avouac, Modelling mountain building and the seismic cycle in the Himalaya of Nepal, J. Geophys. Res. 105 (B6) (2000) 13,389–14,407.
[38] L. Ruff, H. Kanamori, Seismic coupling and uncoupling at subduction zones, Tectonophysics 99 (1983) 99–117.
[39] J.F. Pacheco, L.R. Sykes, C.H. Scholz, Nature of seismic coupling along simple plate boundaries of the subduction type, J. Geophys. Res. 98 (1993) 14,133–14,159.
[40] M. Taylor, G. Zheng, J.R. Rice, W. Stuart, R. Dmowska, Cyclic stressing and seismicity at strongly coupled subduction zones, J. Geophys. Res. 101 (1996) 8363–8382.
[41] R. McCaffrey, C. Goldfinger, Forearc deformation and great subduction earthquakes: implications for Cascadia offshore earthquake potential, Science 267 (1995) 856–859.
[42] J.J. Clague, Evidence for large earthquakes at the Cascadia subduction zone, Rev. Geophys. 35 (1997) 439–460.
[43] M. Chlieh, J. Avouac, K. Sieh, D.H. Natawidjaja, J. Galetzka, Investigating lateral variations of interseismic strain along the Sumatran subduction zone, EOS Trans. AGU 85 (2004) (Fall Meet. Suppl., Abstract T13C-1385).
[44] M. Miller, T. Melbourne, D.J. Johnson, W.Q. Sumner, Periodic slow earthquakes from the Cascadia subduction zone, Science 295 (2002) 2423.
[45] Y. Liu, J.R. Rice, Aseismic slip transients emerge spontaneously in 3D rate and state modeling of subduction earthquake sequences, J. Geophys. Res. 110 (2005) B08307, doi:10.1029/2004JB003424.

[46] D. Natawidjaja, K. Sieh, J. Galetzka, B. Suwargadi, M. Chlieh, H. Cheng, R.L. Edwards, J.P. Avouac, S. Ward, submitted for publication. The giant Sumatran megathrust ruptures of 1797 and 1833: paleoseismic evidence from coral microatolls. J. Geophys. Res.

[47] S. Wiemer, M. Wyss, Minimum magnitude of complete reporting in earthquake catalogs: examples from Alaska, the Western United States, and Japan, Bull. Seism. Soc. Amer. 90 (2000) 859–869.

[48] L. Astiz, T. Lay, H. Kanamori, Large intermediate depth earthquakes and the subduction process, Phys. Earth Planet. Inter. 53 (1988) 80–166.

[49] R. Dmowska, J.R. Rice, L.C. Lovison, D. Josell, Stress transfer and seismic phenomena in coupled subduction zones during the earthquake cycle, J. Geophys. Res. 93 (1988) 7869–7884.

[50] T. Lay, L. Astiz, H. Kanamori, D.H. Christensen, Temporal variation of large interplate earthquakes in coupled subduction zones, Phys. Earth Planet. Inter. 54 (1989) 258–312.

[51] R. Dmowska, G. Zheng, J.R. Rice, Seismicity and deformation at convergent margins due to heterogeneous coupling, J. Geophys. Res. 101 (1996) 3015–3029.

[52] H. Kanamori, D.L. Anderson, Theoretical basis for some empirical relations in seismology, Bull. Seism. Soc. Am. 65 (1975) 1073–1095.

[53] Y. Ogata, Statistical models for earthquake occurrences and residual analysis for point processes, J. Am. Stat. Assoc. 83 (1988) 9–27.

[54] Y. Ogata, Detection of precursory relative quiescence before great earthquakes through a statistical model, J.Geophys. Res. 97 (1992) 19,845–19,871.